Auger Shake-Up Assisted Electron Recapture

M. Žitnik,[1,2] M. Hrast,[1] A. Mihelič,[1,2] K. Bučar,[1,2] J. Turnšek,[1,2] R. Püttner,[3] G. Goldsztejn,[4] T. Marchenko,[4] R. Guillemin,[4] L. Journel,[4] O. Travnikova,[4] I. Ismail,[4] M. N. Piancastelli,[4] M. Simon,[4] D. Ceolin,[5] and M. Kavčič[1,2]

[1]*Jožef Stefan Institute, Jamova cesta 39, SI-1000 Ljubljana, Slovenia*
[2]*Faculty of Mathematics and Physics, University of Ljubljana, Jadranska 31, SI-1000 Ljubljana, Slovenia*
[3]*Fachbereich Physik, Freie Universität Berlin, Arnimallee 14, D-14195 Berlin-Dahlem, Germany*
[4]*Sorbonne Université, UPMC Univ Paris 06, UMR 7614, LCPMR, 75005 Paris, France*
[5]*Synchrotron SOLEIL, L'Orme des Merisiers, Saint Aubin, BP 48, F-91192 Gif-sur-Yvette Cedex, France*

(Received 17 May 2023; revised 6 October 2023; accepted 16 October 2023; published 14 November 2023)

The presence of doubly excited states (DESs) above the core-hole ionization threshold nontrivially modulates the x-ray absorption because the participator Auger decay couples DESs to the underlying low-energy core-hole continuum. We show that coupling also affects the high-energy continuum populated by the spectator Auger decay of DESs. For the $K-L_{23}^2$ Auger decay of the $1s^{-1}3p^{-1}4s^{21}P$ state in argon, the competing nonresonant path is assigned to the recapture of the $1s$ photoelectron caused by emission of the fast electron from the shake-up $K-L_{23}^2$ decay of the $1s^{-1}$ ion.

DOI: 10.1103/PhysRevLett.131.203001

When atoms (A) are exposed to x-ray light and the resulting charge distribution is measured, one sees a drastic change of the signal when photon energy ω crosses the inner-shell ionization threshold. For example, if a peak in the A^+ ion detection channel is observed when the light is tuned to singly excited core-hole state *below* the ionization threshold, it is the yield of A^{2+} ions that increases instead *above* the threshold because an extra (photo)electron is emitted. A closer inspection reveals that the conversion to the A^{2+} ionic species does not occur immediately above the ionization threshold [1–3]. The experiments show that the A^+ yield persists at least a couple of eV above the ionization threshold and that final electronic states of A^+ are the same as those populated by the Auger decay of singly excited states (SESs) converging to the threshold [4–6]. The observed trend is explained by a recapture of the slow photoelectron [4,7,8]: if overtaken soon enough by a faster Auger electron emitted at later times, the photoelectron experiences a rapid change of the potential and loses more than its asymptotic kinetic energy against the Auger electron to become bound again. The recapture is an extreme case of the postcollision interaction (PCI) where, in the simplest and most probable case, the kinetic energy transfer occurs between two electrons in the continuum and causes opposite energy shifts and line asymmetries in the Auger and photoelectron spectra [6,9,10].

We report on a yet unnoticed consequence of PCI, related to atomic doubly excited states (DESs). These resonances are situated tens of eV above the ionization threshold and mostly decay by the core-hole Auger emission. It turns out that due to the PCI, there is a small probability to reach exactly the same final states by the shake-up Auger decay of the underlying core-hole continuum. The same effect is expected to be at work for neutral core-hole resonances in molecules and structures featuring an extra vacancy in the valence shell. It is well-known that DES spectral overlap with the core-hole continuum limits accuracy of the structural information extracted from the photoelectron scattering off the neighboring nuclei [11]. Because of the specific shifts of resonant lines, the spectra of decay products offer the possibility to isolate the scattering part of the absorption spectra [12]. It is thus of a general importance to see how this interesting new decay dynamics imprints on the Auger emission spectra.

The photoelectron recapture can be considered as an extension of the resonant Auger (RA) process $A(0)+\gamma(\omega)\rightarrow A_i\rightarrow A^+(E_f)+e^-(\epsilon_f)$ above the ionization threshold where the intermediate atomic state A_i features one electron in the continuum [13]. The final state of RA is characterized by the kinetic energy ϵ_f of the escaped electron and energy E_f of the residual ion. Most of the experimental RA studies were performed in the near threshold region, and the results were interpreted in the frame of perturbation theory. In these calculations, a number of interfering paths is considered that start by

absorption of a single photon and proceed through one or more bound and/or continuum intermediate atomic states to the A^+ final states as dictated by the Coulomb interaction. The presence of competing paths to the same final states leads to interferences that modulate the spectral features. The number and weights of dominant terms in the expansion of RA amplitude depend on the photon energy: the most direct path with a single intermediate state often prevails when the photon probe is tuned to an isolated atomic resonance. If separately optimized nonorthogonal wave functions are used for description of quantum states, the theory can also explain the observed presence of additional shake-up or shake-down paths where an extra transition of the valence electron is triggered by the Auger decay of the core hole [14]. Approaching the threshold, the density and spectral overlap of resonant states increase and more and more paths contribute to the RA yield. When photon energy is above the threshold, energy detuning of resonances becomes large and intermediate states with photoelectron in the continuum give the largest contribution to the RA amplitude, pointing to the photoelectron recapture as a main source of the signal.

These processes are best studied experimentally by measuring the RA spectral map where the Auger yield is reported as a function of photon energy ω and electron kinetic energy ϵ. Because of the energy conservation, the signal of the A^+ final state occupies a diagonal stripe with $\epsilon_f = \omega - E_f$ on the map and largely avoids the signal of diagram Auger transitions resulting in emission of Auger electrons with characteristic kinetic energies ϵ_A and A^{2+} ions (Fig. 1). In the recent high resolution $K - L_{23}^2$ study of Ar involving $1s^{-1}np$ SESs, the populations of the $2p^{-2}np$ final states up to $n = 7$ were reported by following the RA signal along the corresponding diagonal stripes [15]. The theoretical reconstruction of these constant ionic state (CIS) profiles clearly shows the recapture contribution to the $2p^{-2}5p$ final state, even at photon energies several eV below the ionization threshold.

In this Letter, we study the role of the photoelectron recapture quite far above the $1s$ ionization threshold of argon, in the spectral region of $1s^{-1}3p^{-1}nln'l'$ doubly excited states (DESs). The recapture in this photon energy range starts with the $1s\epsilon p$ continuum and leads most probably to the $Ar^+2p^{-2}nl$ states that are visible in the electron spectrum as weak blue-shifted resonant Raman lines associated with the above mentioned SESs [16]. However, if the photoelectron recapture is accompanied by the shake-up of the $3p$ electron, the same $Ar^+2p^{-2}3p^{-1}nln'l'$ final states are populated as by the $K - L_{23}^2$ Auger decay of DESs. Although such a second-order recapture process may be too weak to be directly observed, it can still have a notable effect on the RA spectrum if it interferes with the resonant process [17].

The simplest case occurs when the recapture competes with the Auger emission from a single resonance.

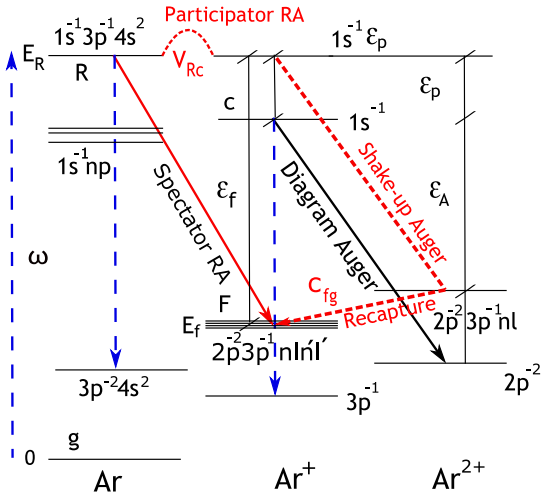

FIG. 1. The electronic transition scheme following photon absorption in the region of $1s^{-1}3p^{-1}4s^2$ DESs in argon. V_{Rc} denotes amplitude of the $R \to 1s^{-1}\epsilon p$ participator Auger decay to the low-energy continuum. The spectator Auger decay (red arrow) couples R to the high-energy $2p^{-2}3p^{-1}nln'l'\epsilon(s,d)$ continuum, which is populated also by the Auger shake-up assisted photoelectron recapture from the low-energy continuum (dotted red arrow, c_{fg} amplitude). The dashed (blue) arrows and the black arrow mark the $K - M$ x-ray decay and the diagram $K - L_{23}^2$ Auger decay, respectively. The kinetic energies of the $1s$ photoelectron and of the resonant and nonresonant $K - L_{23}^2$ electrons are denoted by ϵ_p, ϵ_f, and ϵ_A, respectively. For clarity, the $K - L$ decay is omitted.

To approach this condition, the photon energy was scanned across an isolated DES in Ar, the so-called conjugate shake-up resonance R with excitation energy $E_R = 3222.4$ eV [18] (Fig. 1). This weak $^1P_1$ state is described by the 9:1 mixture of $1s^{-1}3p^{-1}4s^2$ and $1s^{-1}3p^{-1}4p^2$ configurations, and lies 16.5 eV above the K-shell ionization threshold and 6.2 eV below the first $1s^{-1}3p^{-1}4p$ shake-up threshold [12]. The neighboring DESs with a significant oscillator strength have at least 2.7 eV higher excitation energy. Resonance R features 1-fs lifetime corresponding to the natural broadening $\Gamma = 0.68$ eV, and predominantly decays by the $K - L^2$ Auger (77%) and $K - L$ x-ray emission (12%) [19–21].

When the interference is absent, an isolated character of resonance R suggests a simple $[(\omega - E_R)^2 + \Gamma^2]^{-1}$ Lorentzian dependence of the yield of decay products before the convolution with the photon probe profile. Indeed, our previous resonant inelastic x-ray scattering (RIXS) study has verified a symmetric Voigt profile of the $K - M_{23}$ x-ray yield emitted by this resonance [12]. Similar to RIXS, the shift of the kinetic energy of RA electrons allows one to separate the RA signal from an intense Auger emission of Ar^+1s^{-1} ions. In Fig. 2, the nonresonant $K - L_{23}^2$ Auger spectrum at 3219.4 eV photon energy is compared to the Auger spectrum recorded at $\omega = E_R$. An

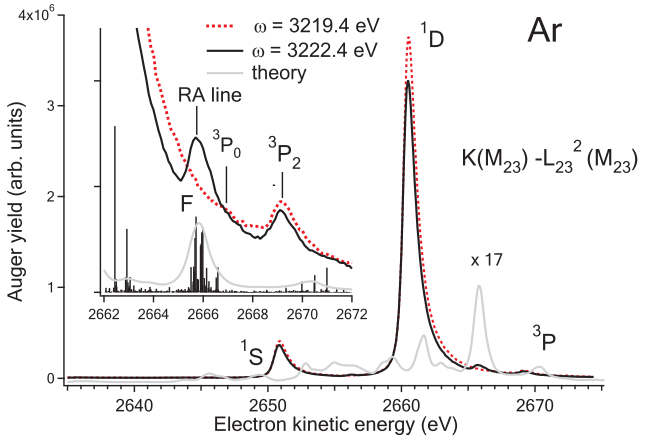

FIG. 2. The $K(M) - L_{23}^2(M)$ electron yield of Ar measured at 3219.4 eV (red dotted curve) and 3222.4 eV (black curve) photon energy. The inset shows the RA line emitted by the $1s^{-1}3p^{-1}4s^2$ atomic resonance and two weak $^3P_{2,0}$ nonresonant Auger lines emitted in decay of the $1s^{-1}$ state. The corresponding theoretical RA spectrum (gray curve) is shifted and scaled to match the observed position and intensity of the observed RA line, respectively. The bars show relative contributions of final states to an angle-integrated RA spectrum. Label F denotes a group of final states giving rise to the RA line.

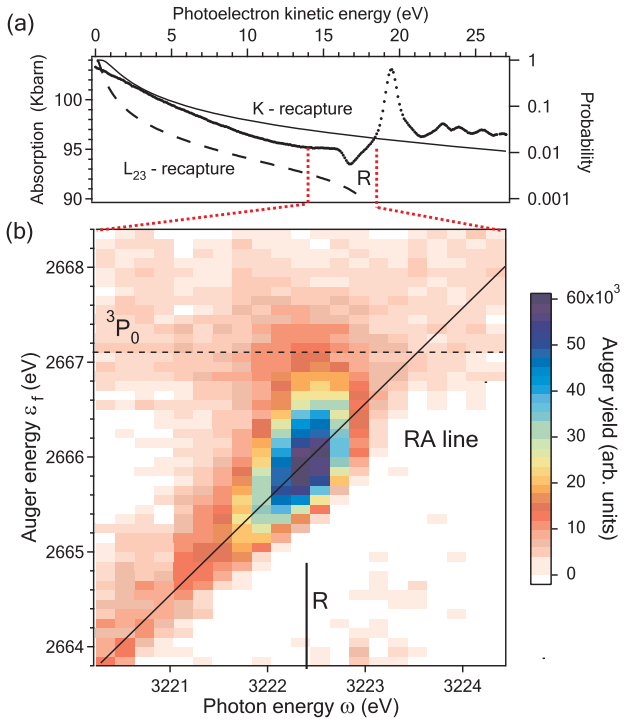

FIG. 3. (a) The measured absorption spectrum (black dots) in the region of the $1s^{-1}3p^{-1}nln'l'$ DES in Ar [12]. According to the semiclassical estimate [see Eq. (9) in Ref. [4]], the recapture more likely occurs due to emission of faster $K - L^2$ Auger electrons (black curve) than slower $L - M^2$ Auger electrons (black dotted curve) at the same asymptotic kinetic energy of photoelectron. (b) The $K(M) - L_{23}^2(M)$ electron yield in the vicinity of resonance R leading to final states F after subtracting the tail of the $2p^{-2}{}^1D_2$ diagram Auger line. The RA line shows a linear dispersion (black line), while the position of the weak $2p^{-2}\ ^3P_0$ diagram line is independent of photon energy (dashed line).

additional line at $\epsilon = 2665.8$ eV clearly pops up on the high energy tail of the ^1D diagram line under the resonant condition, showing that the RA paths mediated by resonance R populate the group F of $Ar^+2p^{-2}3p^{-1}nln'l'$ final states with the binding energies $E_f \approx 556.5$ eV. A magnified view of the spectral region also shows the presence of weak $^3P_2$ and $^3P_0$ diagram Auger lines positioned at 2669.1 and 2667.1 eV, respectively [19].

We have built up the RA map in the region of resonance R by stacking a sequence of well-resolved $K(M_{23}) - L_{23}^2(M_{23})$ electron spectra covering the 3220.2–3224.4 eV photon energy range with a 0.2-eV step [see Fig. 3(b)]. The experiment was performed at the GALAXIES beamline at the SOLEIL synchrotron in France (see Ref. [22] for details). The RA yield mediated by resonance R and associated with the occupation of final states F shows the expected linear Raman dispersion and an unexpected asymmetry with respect to the photon energy. The CIS spectrum of F in Fig. 4(b) is obtained by integrating the corresponding RA line over the Auger electron kinetic energy ϵ_f and subtracting the constant contribution of $2p^{-2}\ ^3P_0$ diagram line. The corresponding CIS profile is different from the symmetric CIS profile extracted from the RIXS spectral map [Fig. 4(a)] and encourages an explanation in terms of a single resonance R interfering with the continuum—the Fano resonance [23]. We claim that the continuum amplitude comes from the combined action of $K - L_{23}^2$ shake-up Auger decay and photoelectron recapture from the $1s^{-1}\epsilon p$ continuum. Note that for *singly excited* intermediate states, the CIS asymmetry may be also caused by the interference of the RA amplitude with the nonresonant photoionization amplitude populating the same final ionic states directly from the atomic ground state [24,25]. However, such a direct photoionization process is of a minor importance for Auger spectroscopy of DESs.

Indeed, the recent state-of-the-art spectroscopic study of argon with 3216 eV photons has shown that $(4.8 \pm 1.0)\%$ of the nonresonant $K - L_{23}^2$ transitions are accompanied by the $3p$ electron jump to the higher orbital populating primarily the $Ar^{2+}2p^{-2}3p^{-1}4p$ final states [26]. The corresponding Auger electrons are thus observed at lower kinetic energies than the characteristic $K - L_{23}^2$ electrons. On the other hand, for the short-lived K-hole states emitting 2.6 keV Auger electrons, the semiclassical model estimates 2.4% probability to recapture the 16.5-eV photoelectron [4]. It may be that some of the Auger electrons are involved in both the energy losing shake-up *and* energy gaining photoelectron recapture. Neglecting the angular

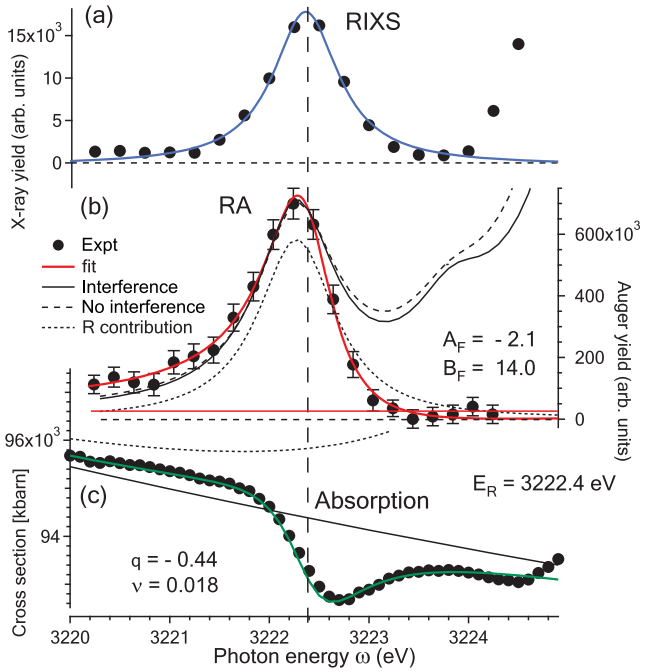

FIG. 4. The three faces of the $1s^{-1}3p^{-1}4s^2$ resonance in Ar. (a) The resonance profile constructed from x-ray yield of the $K-M_{23}$ satellite line (black points), fitted by the Lorentzian (blue curve) [12]. (b) The profile constructed from the electron yield of the $K-L_{23}^2$ satellite line F (black points), fitted by Eq. (1) (red curve). The comparison is made with the calculated CIS, considering (black curve) and not considering (black dashed curve) the interferences with DES neighbors. The dotted black curve presents the calculated contribution of resonance R. (c) The absorption spectrum (black points) fitted by the sum (green curve) of the Fano profile and the noninteracting continuum background [see Eq. (A5) in the Appendix]. The extrapolated background of the unperturbed $1s\epsilon p$ photoionization without (black curve) and with added contribution of the higher-lying resonances (black dotted curve) are also plotted.

momentum exchange between the slow photoelectron and fast Auger electron, the shake-up recapture interferes with the spectator RA because both paths populate the same final continuum states f. Without resorting to extended quantum many-body calculations, the best estimate for the conversion probability of the $1s^{-1}\epsilon p$ to the $2p^{-2}3p^{-1}nln'l'\epsilon(s,d)$ continuum is $(11.5\pm2.4)\times10^{-4}$ at $\omega=E_R$ and is given by the product of $1s^{-1}$ shake-up Auger decay probability (4.8%) and photoelectron recapture probability (2.4%).

We need to see whether this estimate is consistent with the observed CIS profile in Fig. 4(b). Since the photon energy dependence of the nonresonant amplitude is dictated by the shake-up Auger emission and photoelectron recapture probability, the corresponding c_{fg} amplitudes are practically constant in the region of resonance R. This assumption would remain valid even when c_{fg} comprises some contribution of the shake-up RA paths mediated by spectrally distant SESs. However, our calculations show that at 19 eV detuning, the shake-up RA amplitudes mediated by the dominant $1s4p^{-1}$ resonance are too small to explain the profile's asymmetry. The calculations also show that RA paths through much closer higher-lying DESs cannot explain the observed CIS deviation from the Lorentz profile because their interference with the RA paths involving R is too weak [Fig. 4(b)]. Note that the atomic and ionic states with several open (valence) shells are highly correlated. To interpret our measurements, we have performed a multiconfiguration Dirac-Fock calculation showing that in the selected spectral frame, the whole group of final states F is populated by the Auger decay of resonance R (see Fig. 2 inset) and that the corresponding Auger emission is practically isotropic [22].

The nonresonant amplitudes c_{fg} of all paths to final states f in the F group *except the paths through resonance* R are thus approximately independent of photon energy in the resonance region. To interpret the observed CIS spectrum, we need to sum the photoionization cross sections for all final states f in the range of peak F (see Fig. 2 inset). The individual cross sections are parametrized as explained in the past [27,28], only that now the dipole photoionization amplitude from the ground state g to the single-electron continuum f is replaced by c_{fg} amplitude that describes the transition as a combined effect of photoionization, shake-up Auger emission, and photoelectron recapture. In summary, the CIS profile

$$F(x)\propto 1+\frac{2xA_F+B_F}{1+x^2} \tag{1}$$

depends on the dimensionless photon energy detuning $x=2(\omega-E_R)/\Gamma$ and on parameters A_F and B_F obtained by averaging over the final continuum channels f (see Appendix). The form (1) matches the observed CIS profile very well when $A_F=-2.1\pm0.5$ and $B_F=14.0\pm0.9$ [Fig. 4(b)]. While A_F describes the observed CIS asymmetry, B_F gives the probability ratio for an electron to originate in the resonant or the nonresonant path at zero photon energy detuning.

The knowledge of B_F offers an independent way to estimate the relative probability to reach final states F by the nonresonant process if P_R, the photoexcitation probability of the selected DES with respect to the $1s^{-1}\epsilon p$ continuum, is known. Unfortunately, the photoabsorption profile of R is not far from the Fano window resonance [[23]; see Fig. 3(a)]. This prevents a reliable determination of P_R because the photoabsorption amplitude to the unperturbed state is almost canceled by the amplitude modification due to the interacting continuum, which is activated by the participator Auger decay $R\rightarrow \mathrm{Ar}^+1s^{-1}+e^-$. When the same resonance is observed in the RIXS decay channel, such interference effects are absent and the signal of the weak atomic $K-M_{23}$ x-ray satellite line is separable from the

$K-M_{23}$ diagram line emitted by Ar^+1s^{-1} ions. Taking the ratio of the two measured x-ray yields at $\omega = E_R$, one finds $P_R = (1.5 \pm 0.2)\%$, after accounting for a small difference between the calculated atomic and ionic $K-M_{23}$ emission oscillator strengths (see Fig. 1 in Ref. [12]). Based on a known $K-L_{23}^2$ branching ratio for Ar [19] and using the calculated $K-L_{23}^2$ RA spectrum, we estimate that resonance R decays to the group of final states F with 24% probability. Finally, multiplying this probability by P_R/B_F one obtains $(2.6 \pm 0.6) \times 10^{-4}$ for the probability to populate final states F from the $1s^{-1}\epsilon p$ continuum. Although this is about 4 times smaller than our previous estimate of the shake-up Auger assisted photoelectron recapture probability, the two probabilities are still consistent because the simple product estimate is not limited to the group of final states F. These results suggest that in about 77% of cases the photoelectron recapture ends in the $Ar^+2p^{-2}3p^{-1}nln'l'$ final states outside the group F. It is quite hopeless to detect the corresponding spectral effects because at photon energy E_R these states are weakly populated from the resonance R and/or their signal is masked by the diagram Auger lines (see Fig. 2).

In conclusion, we have presented a new general interference scheme that can significantly disturb the separation of DES absorption signal from the underlying electron continuum even if the corresponding features are clearly separated in the resonant Auger spectra. The resonant $K-L_{23}^2$ Auger decay of DESs was found to interfere with a weak nonresonant process that converts the $1s^{-1}\epsilon p$ low-energy electron continuum to the $2p^{-2}3p^{-1}nln'l'\epsilon(s,d)$ high-energy continuum. The nonresonant process involves three active electrons and is driven by a combination of the shake-up $K-L_{23}^2$ Auger decay of the Ar^+1s^{-1} ion and recapture of the $1s$ photoelectron. At 16.5 eV above the $1s$ ionization threshold of argon, *one per thousand* of $K-L_{23}^2$ decays is redirected from Ar^{2+} to Ar^+ decay channel by the Auger shake-up assisted photoelectron recapture. The same mechanism is expected to be at work in other atomic and molecular systems, too, with a relative probability depending on the core-hole lifetime, shake-up Auger probability, and initial kinetic energies of photoelectron and Auger electron. In general, the attempts to separate resonant part of the absorption from the continuum have limited accuracy as soon as these two components interfere in at least one of the decay channels.

This work was financially supported by the Slovenian Research Agency in the framework of the P1-0112 research program "Studies of Atoms, Molecules and Structures by Photons and Particles." We are grateful to the SOLEIL staff for their operation of the facility. We thank the XAFS beamline staff at Elettra for the assistance in acquiring the absorption spectrum at argon K-edge. The authors acknowledge the HPC RIVR consortium and SLING for providing the computing resources of the HPC systems Arnes, NSC and Trdina.

Appendix: On parametrization.—Resonant Auger emission in the presence of shake-up Auger assisted photoelectron recapture: The CIS spectrum in Fig. 4(b) is described by a sum of photoionization cross sections σ_f to final states f in the F group (see the inset of Fig. 2). Each of the cross sections is proportional to the yield of electrons with kinetic energy ϵ_f emitted at photon energy ω and can be written as

$$\sigma_f(x) \propto |c_{fg}|^2 \left(\frac{x^2 + 2A_f x + B_f}{x^2 + 1} \right). \tag{A1}$$

The above form assumes that the final state is populated either by the $K-L_{23}^2$ Auger decay of resonance R or nonresonantly, as described by the amplitude c_{fg} [27,28] and depends on the dimensionless photon energy detuning $x = 2(\omega - E_R)/\Gamma$. The real parameters A_f and B_f are defined by Eq. (26) of Ref. [27] in terms of the Fano parameter and the complex parameter α_f [29]. The formal expressions for these two quantities are found in Ref. [27] provided that the dipole amplitudes for a direct transition from the ground state (g) to the final continuum states (f) in Eqs. (22) and (24) are replaced by the corresponding amplitudes c_{fg} describing the nonresonant transition as a combined effect of photoionization, shake-up Auger emission, and photoelectron recapture from the atomic ground state. Parameter α_f thus represents the fraction of c_{fg}, which passes through a single eigenchannel interacting with a discrete state that is embedded in several continua (see Ref. [23]). Performing summation of (A1) over the group F of final states, the fitting form (1) emerges where

$$A_F = \sum_f^F A_f |c_{fg}|^2 / \sum_f^F |c_{fg}|^2, \tag{A2}$$

$$B_F = \sum_f^F (B_f - 1) |c_{fg}|^2 / \sum_f^F |c_{fg}|^2, \tag{A3}$$

are the averages of A_f and $B_f - 1$ over the selected continuum channels.

Absorption in the presence of resonance coupled to low-energy and high-energy continua: When a discrete state is coupled to several continua that are orthogonal themselves, the problem can be reduced by transforming the continua to a new basis in which the state interacts with one continuum only and the rest of the continua are noninteracting. For two orthogonal continua, the transformation has been worked out in the paper of Fano [23] and Eqs. (40)–(44) are directly

applicable for parametrization of the Ar $1s$ photoionization cross section in the region of an isolated DES.

In our case, a DES is coupled to one low-energy continuum and several high-energy continua. When photon energy is set to the resonance energy $E_R = 3222.4$ eV, the low-energy continuum coincides with the $1s^{-1}\epsilon p$ continuum where the $1s$ photoelectron features 16.5 eV kinetic energy. In addition to the direct ground state photoionization, the low-energy continuum is populated by the $1s$-hole-preserving participator Auger decay of DESs characterized by Γ_v rate. The high-energy continua are populated by the spectator Auger decay of DESs where the $1s$ vacancy is filled by $K-L^2$, $K-LM$, and $K-M^2$ Auger transitions with the total decay rate Γ_A and an electron with at least 2.5 keV kinetic energy is emitted. These high-energy continua can be treated as one because none of them can be reached by a direct single-photon ionization of atoms in the ground state. In effect, when $\Gamma_v \ll \Gamma_A$, the interacting continuum contains only a small part of the low-energy continuum and its major part resides in the noninteracting continuum. Thus, the photoionization cross section is described by the sum of two terms weighted in proportion to $\nu = \Gamma_v/\Gamma_A$: a well-known but small contribution of the one discrete state-one continuum Fano term characterized by Fano parameter q' and a large quasiconstant contribution due to photoexcitation of the low-energy continuum component of the noninteracting continuum. Denoting direct photoionization amplitude to the low-energy continuum by D_{vg} and introducing $x' = 2(\omega - E_R)/(\Gamma_v + \Gamma_A)$, the cross section is expressed by

$$\sigma'_{\text{ion}} \propto |D_{vg}|^2 \left(\frac{\nu}{1+\nu} \frac{(x'+q')^2}{x'^2+1} + \frac{1}{1+\nu} \right). \quad \text{(A4)}$$

Since DESs also emit x-rays with decay rate Γ_r, Eq. (A4) must be modified to describe photoionization cross section in the presence of radiative dumping [30]. Denoting by $\Gamma = \Gamma_v + \Gamma_A + \Gamma_r$ the total decay rate of DESs, the Fano parameter q' is replaced by $q = q'(\Gamma_v + \Gamma_A)/\Gamma$, energy detuning $x = 2(\omega - E_R)/\Gamma$ replaces x' and the Lorentzian, proportional to $\mu^2 = \Gamma_r^2/\Gamma^2$, must be added to (A4):

$$\sigma_{ion} \propto |D_{vg}|^2 \left(\frac{\nu}{1+\nu} \frac{(x+q)^2+\mu^2}{x^2+1} + \frac{1}{1+\nu} \right). \quad \text{(A5)}$$

Equation (A5) with $q = -0.44 \pm 0.05$ and $\nu = 0.018 \pm 0.002$ fits well the experimental absorption spectrum in Fig. 4(c). The presence of the Lorentzian with $\mu = 0.12$ does not significantly affect the fitting result. Prior to the fitting, a smooth $|D_{vg}|^2$ ionization background was estimated by extrapolation of the measured absorption signal from below the resonance region and most of the contribution of higher-lying resonances was subtracted. In principle, to construct the absorption cross section, $\mu P_R |D_{vg}|^2/(x^2+1)$ must be added to (A5) to account for x-ray decay of DESs. However, the contribution of this term is small and does not affect parameter values beyond the assigned error bars.

We have nearly reproduced the ν value from the fit by calculations: the ratio of the participator Auger rate $\Gamma_v = 7.7$ meV versus Γ_A (estimated from the calculated $K-L_{23}^2$ Auger decay rate of DESs [19,22]) is 0.016. The calculation of q parameter is out of the scope of this work because, for the windowlike resonances, the coupling of a discrete state with the continuum has to be carefully evaluated over a large range of photoelectron energies.

Note that shake-up Auger assisted photoelectron recapture, the main subject of this Letter, does not affect the above analysis. The recapture couples only weakly the low-energy and high-energy continua and can be safely neglected to model the absorption profile. On the other hand, a relatively weak participator Auger coupling does not affect significantly the nonresonant recapture paths to the high-energy continua because it generates only a small modification of the low-energy continuum.

[1] W. Eberhardt, S. Bernstorff, H. W. Jochims, S. B. Whitfield, and B. Crasemann, Phys. Rev. A **38**, 3808 (1988).
[2] K. Ueda, E. Shigemasa, Y. Sato, A. Yagishita, M. Ukai, H. Maezawa, T. Hayaishi, and T. Sasaki, J. Phys. B **24**, 605 (1991).
[3] J. Doppelfeld, N. Anders, B. Esser, F. von Busch, H. Scherer, and S. Zinz, J. Phys. B **26**, 445 (1993).
[4] X. Feng, A. A. Wills, E. Sokell, T. W. Gorczyca, M. Wiedenhoeft, and N. Berrah, Phys. Rev. A **72**, 042712 (2005).
[5] U. Hergenhahn, A. D. Fanis, G. Prümper, A. K. Kazansky, N. M. Kabachnik, and K. Ueda, J. Phys. B **38**, 2843 (2005).
[6] R. Guillemin, S. Sheinerman, R. Püttner, T. Marchenko, G. Goldsztejn, L. Journel, R. K. Kushawaha, D. Céolin, M. N. Piancastelli, and M. Simon, Phys. Rev. A **92**, 012503 (2015).
[7] G. B. Armen, J. C. Levin, and I. A. Sellin, Phys. Rev. A **53**, 772 (1996).
[8] S. A. Sheinerman, J. Phys. B **38**, 2279 (2005).
[9] M. U. Kuchiev and S. A. Sheĭnerman, Sov. Phys. Usp. **32**, 569 (1989).
[10] V. Schmidt, Rep. Prog. Phys. **55**, 1483 (1992).
[11] D. E. Sayers, E. A. Stern, and F. W. Lytle, Phys. Rev. Lett. **27**, 1204 (1971).
[12] M. Kavčič, M. Žitnik, K. Bučar, A. Mihelič, M. Štuhec, J. Szlachetko, W. Cao, R. Alonso Mori, and P. Glatzel, Phys. Rev. Lett. **102**, 143001 (2009).
[13] G. B. Armen, H. Aksela, T. Åberg, and S. Aksela, J. Phys. B **33**, R49 (2000).
[14] J. A. de Gouw, J. van Eck, A. C. Peters, J. van der Weg, and H. G. M. Heideman, J. Phys. B **28**, 2127 (1995).
[15] D. Céolin, T. Marchenko, R. Guillemin, L. Journel, R. K. Kushawaha, S. Carniato, S.-M. Huttula, J. P. Rueff, G. B. Armen, M. N. Piancastelli, and M. Simon, Phys. Rev. A **91**, 022502 (2015).

[16] M. Žitnik, R. Püttner, G. Goldsztejn, K. Bučar, M. Kavčič, A. Mihelič, T. Marchenko, R. Guillemin, L. Journel, O. Travnikova, D. Céolin, M. N. Piancastelli, and M. Simon, Phys. Rev. A **93**, 021401(R) (2016).
[17] B. Krässig, E. P. Kanter, S. H. Southworth, R. Guillemin, O. Hemmers, D. W. Lindle, R. Wehlitz, and N. L. S. Martin, Phys. Rev. Lett. **88**, 203002 (2002).
[18] S. Svensson, B. Eriksson, N. Mårtensson, G. Wendin, and U. Gelius, J. Electron Spectrosc. Relat. Phenom. **47**, 327 (1988).
[19] L. Asplund, P. Kelfve, B. Blomster, H. Siegbahn, and K. Siegbahn, Phys. Scr. **16**, 268 (1977).
[20] M. O. Krause, J. Phys. Chem. Ref. Data **8**, 307 (1979).
[21] M. O. Krause and J. H. Oliver, J. Phys. Chem. Ref. Data **8**, 329 (1979).
[22] M. Žitnik *et al.*, companion article, Phys. Rev. A **108**, 053113 (2023).
[23] U. Fano, Phys. Rev. **124**, 1866 (1961).
[24] N. Martensson, S. Svensson, and U. Gelius, J. Phys. B **20**, 6243 (1987).
[25] R. Camilloni, M. Žitnik, C. Comicioli, K. C. Prince, M. Zacchigna, C. Crotti, C. Ottaviani, C. Quaresima, P. Perfetti, and G. Stefani, Phys. Rev. Lett. **77**, 2646 (1996).
[26] R. Püttner, P. Holzhey, M. Hrast, M. Žitnik, G. Goldsztejn, T. Marchenko, R. Guillemin, L. Journel, D. Koulentianos, O. Travnikova, M. Zmerli, D. Céolin, Y. Azuma, S. Kosugi, A. F. Lago, M. N. Piancastelli, and M. Simon, Phys. Rev. A **102**, 052832 (2020).
[27] A. F. Starace, Phys. Rev. A **16**, 231 (1977).
[28] I. Sánchez and F. Martin, Phys. Rev. A **44**, 7318 (1991).
[29] U. Fano and J. W. Cooper, Phys. Rev. **137**, A1364 (1965).
[30] F. Robicheaux, T. W. Gorczyca, M. S. Pindzola, and N. R. Badnell, Phys. Rev. A **52**, 1319 (1995).